Synthesis and Characterization of Novel Low-Bandgap Triphenylamine-Based Conjugated Polymers with Main-Chain Donors and Pendent Acceptors for Organic Photovoltaics

DURYODHAN SAHU,[1] HARIHARA PADHY,[1] DHANANJAYA PATRA,[1] JEN-HSIEN HUANG,[2] CHIH-WEI CHU,[2,3] HONG-CHEU LIN[1]

[1]Department of Materials Science and Engineering, National Chiao Tung University, Hsinchu, Taiwan, Republic of China

[2]Research Center for Applied Sciences, Academia Sinica, Taipei, Taiwan, Republic of China

[3]Department of Photonics, National Chiao Tung University, Hsinchu, Taiwan, Republic of China

Received 17 August 2010; accepted 13 September 2010
DOI: 10.1002/pola.24389
Published online 22 October 2010 in Wiley Online Library (wileyonlinelibrary.com).

ABSTRACT: A series of novel low-bandgap triphenylamine-based conjugated polymers (**PCAZCN**, **PPTZCN**, and **PDTPCN**) consisting of different electron-rich donor main chains (*N*-alkyl-2,7-carbazole, phenothiazine, and cyclopentadithinopyrol, respectively) as well as cyano- and dicyano-vinyl electron-acceptor pendants were synthesized and developed for polymer solar cell applications. The polymers covered broad absorption spectra of 400–800 nm with narrow optical bandgaps ranging 1.66–1.72 eV. The highest occupied molecular orbital and lowest unoccupied molecular orbital levels of the polymers measured by cyclic voltammetry were found in the range of −5.12 to −5.32 V and −3.45 to −3.55 eV, respectively. Under 100 mW/cm^2 of AM 1.5 white-light illumination, bulk heterojunction photovoltaic devices composing of an active layer of electron-donor polymers (**PCAZCN**, **PPTZCN**, and **PDTPCN**) blended with electron-acceptor [6,6]-phenyl-C_{61}-butyric acid methyl ester or [6,6]-phenyl-C_{71}-butyric acid methyl ester ($PC_{71}BM$) in different weight ratios were investigated. The photovoltaic device containing donor **PCAZCN** and acceptor $PC_{71}BM$ in 1:2 weight ratio showed the highest power conversion efficiency of 1.28%, with $V_{oc} = 0.81$ V, $J_{sc} = 4.93$ mA/cm^2, and fill factor = 32.1%. © 2010 Wiley Periodicals, Inc. J Polym Sci Part A: Polym Chem 48: 5812–5823, 2010

KEYWORDS: bulk heterojunction; conducting polymers; conjugated polymers; donor–acceptor; heteroatom-containing polymers; low bandgap; polymer solar cells; synthesis; triphenylamine derivatives

INTRODUCTION

Solar cells based on polymers have attracted intense research interests in recent years because of their unique advantages of low cost, light weight, and compatibility for making flexible and large area devices.[1] To date, solution-processed bulk heterojunction (BHJ) polymer solar cell (PSC) devices composed of an active layer of electron-donor polymers blended with electron-acceptor fullerene derivatives, such as [6,6]-phenyl-C_{61}-butyric acid methyl ester ($PC_{61}BM$) or [6,6]-phenyl-C_{71}-butyric acid methyl ester ($PC_{71}BM$), have been developed and reached power conversion efficiency (PCE) values up to 7.7%.[2–4] Moreover, the PSC devices with appropriate industrial processing technique of traditional silicon-based solar cells have also been extended.[5] Nevertheless, unlike silicon-based solar cells, these PCEs of PSC devices are not sufficient for commercialization, though there are lot of advantages of polymers. To seek higher efficiencies, there have been various research efforts focused on the design and synthesis of polymers with new electron-rich and electron-deficient units along their backbones.[6–20] In general, to acquire higher PCE values in BHJ solar cells, the developments of new materials were focused on: (i) fused aromatic rings in the conjugated polymer backbones that endow with strong absorption spectra, which can harvest more sunlight in the whole solar spectrum,[6–8] to increase the J_{sc} values; (ii) tunable intramolecular charge transfer (ICT) from electron-donor to electron-acceptor units that lower the bandgaps;[9–11] (iii) the minimum difference (should be 0.3 eV) between the highest occupied molecular orbital (HOMO) level of the polymer and the lowest unoccupied molecular orbital (LUMO) level of the PCBM acceptor in the active layer, which provides an efficient driving force for the charge separation to get a high open circuit voltage (V_{oc});[6(d,e),12,14] and (iv) the excited electron-hole pairs need to be dissociated into free charge carriers with high yields.[3(a)]

During the last decade, many articles have been reported based on conjugated polymers with electron-donating and electron-accepting moieties combined through π-conjugated linkers in the polymer backbones, which reduce the optical bandgaps and allow the absorptions of the polymers to match well with the solar spectrum.[16–19] In donor–acceptor

Additional Supporting Information may be found in the online version of this article. Correspondence to: H.-C. Lin (E-mail: linhc@mail.nctu.edu.tw)

(D-A) polymers, the electron-donor units provide deeper HOMO levels, and the electron-acceptor units are responsible for the electronic bandgaps of the polymers.[20] Furthermore, to get high PCE values, the strategy to design conjugated polymers, where the electron-acceptors were placed at the pendants connected with electron-rich main chains, was found to be evenly effective and showed promising performances with PCE values up to 4.5%.[21] These architectures composing of electron-acceptor pendants and electron-donor main chains have the unique advantages of allowing charge separation through sequential transfers of electrons from the main chains to the side chains and then to PCBM, though there are limited reports explored in PSC applications.[21] Numerous conjugated units, such as 2,7-carbazole,[6] cyclopentadithiophene,[7] cyclopentadithinopyrol,[8(a–c)] phenothiazine,[9(c–e)] and triphenylamine[10,21(a–c)] containing electron-rich heteroatoms (i.e., N, S, and Si), have been extensively used in the polymer designs for the applications of PSCs. As a donor moiety, 2,7-carbazole derivatives showed both smaller bandgaps and deeper HOMO energy levels, which enabled higher light harvestings and V_{oc} values (up to 0.9 V), respectively.[6] For instance, Heeger et al. reported that a polymer (PCDTBT) containing 2,7-carbazole as a donor moiety showed a PCE value of 6.1% along with the best ever internal quantum efficiency of 100%.[6(c)] Moreover, the introduction of alkyl chains in donor moieties of polymers provides good balance between solubility and crystallinity in polymer films and also has impacts on PCE values.[22] Furthermore, the introduction of electron-withdrawing cyano- or dicyanovinyl groups to polymer backbones lowers their LUMO levels,[23] tunes their electrooptical properties,[11,24] and also enhances their electrochemical stabilities.[10(b),25]

In this study, we report the synthesis and characterization of three novel low-bandgap D-A triphenylamine-based conjugated polymers (**PCAZCN**, **PPTZCN**, and **PDTPCN**), where a triphenylamine derivative (**M1**) bearing an electron-withdrawing cyano- and dicyano-vinyl pendant was copolymerized with three different electron-rich donor (**M2**–**M4**) blocks, those are, *N*-alkyl-2,7-carbazole, -3,7-phenothiazine, and -2,6-dithinopyrol, respectively, via Suzuki and Stille reactions (see Fig. 1 and Schemes 1 and 2). These highly electron-rich donor groups, including triphenylamine derivative (**M1**)[21(c),26] and electron-donor blocks **M2–M4**, in the backbones of the main-chain copolymers endowed with strong and broad absorption spectra to obtain superior harvesting of sunlight and also suitable molecular energy levels to acquire good charge separations and transportations as well as high values of V_{oc}. Solution-processed BHJ PSC devices composed of an active layer of electron-donor polymers blended with electron-acceptor $PC_{61}BM$ or $PC_{71}BM$ were developed, and their photovoltaic properties were investigated as well.

EXPERIMENTAL

Materials

4-(Tridecan-7-yl)-4H-dithieno[3,2-b:2′,3′-d]pyrrole was prepared according to the published procedure.[8(c)] All other chemicals were purchased from Aldrich, ACROS, Fluka, or TCI. Toluene, tetrahydrofuran (THF), and diethyl ether were distilled over sodium/benzophenone. Chloroform ($CHCl_3$) was purified by refluxing with calcium hydride and then distilled. If not otherwise specified, the other solvents were degassed by nitrogen 1 h before use.

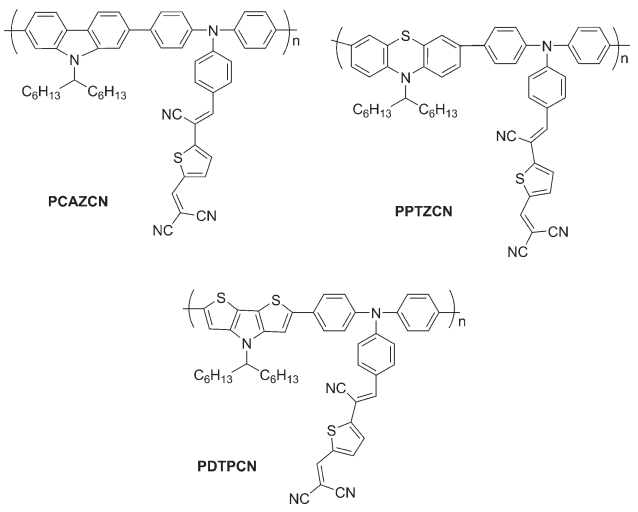

FIGURE 1 Molecular structures of polymers (**PCAZCN**, **PPTZCN**, and **PDTPCN**).

Measurements and Characterization

^1H and ^{13}C NMR spectra were measured using Varian Unity 300 MHz spectrometer. Elemental analyses were performed on a HERAEUS CHN-OS RAPID elemental analyzer. Thermogravimetric analyses (TGA) were conducted with a TA Instruments Q500 at a heating rate of 10 °C/min under nitrogen. The molecular weights of polymers were measured by gel permeation chromatography (GPC) using Waters 1515 separation module (concentration: 1 mg/1 mL in THF; flow rate: 1 mL/1 min), and polystyrene was used as a standard with THF as an eluent. UV–visible absorption spectra were recorded in dilute THF solutions (10^{-6} M) on a HP G1103A. Solid films of UV–vis spectra measurements were spin coated on a glass substrate from THF solutions with a concentration of 10 mg/mL. Cyclic voltammetry (CV) measurements were performed using a BAS 100 electrochemical analyzer with a standard three-electrode electrochemical cell in a 0.1 M tetrabutylammonium hexafluorophosphate solution (in acetonitrile) at room temperature with a scanning rate of 100 mV/s. During the CV measurements, the solutions were purged with nitrogen for 30 s. In each case, a carbon working electrode coated with a thin layer of polymers, a platinum wire as the counter electrode, and a silver wire as the quasi-reference electrode were used, and Ag/AgCl (3 M KCl) electrode was served as a reference electrode for all potentials quoted herein. The redox couple of ferrocene/ferrocenium ion (Fc/Fc^+) was used as an external standard. The corresponding HOMO and LUMO levels were calculated using $E_{ox/onset}$ and $E_{red/onset}$ for experiments in solid films of polymers, which were performed by drop-casting films with the similar thickness from THF solutions (ca. 5 mg/mL). The onset potentials were determined from the intersections of two tangents

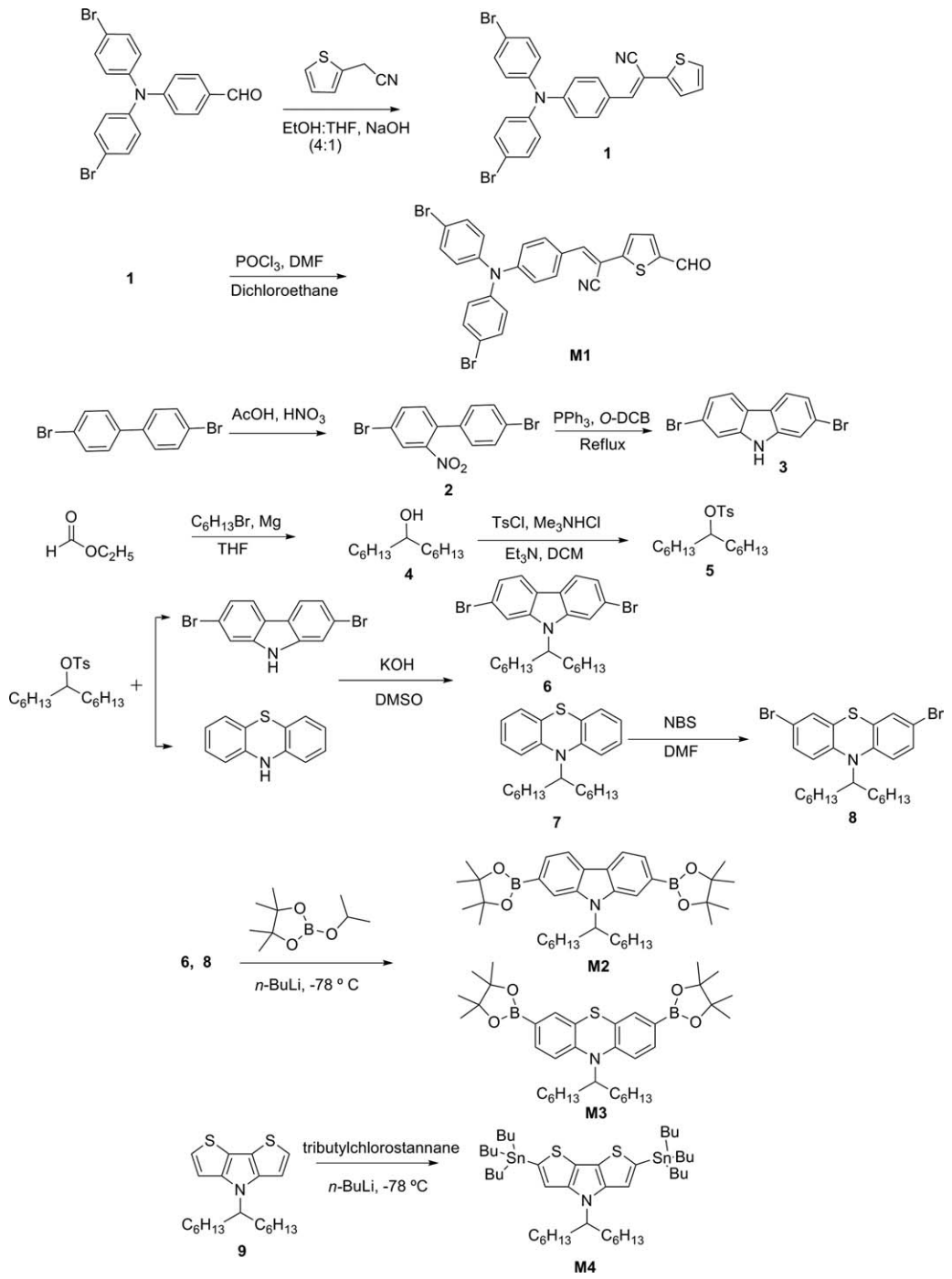

SCHEME 1 Synthetic routes of monomers (**M1–M4**).

drawn at the rising currents and background currents of the CV measurements.

Fabrication of PSCs

The PSCs in this study were composed of an active layer of blended polymers (polymer:PCBM) in solid films, which were sandwiched between a transparent indium tin oxide (ITO) anode and a metal cathode. Before the device fabrication, ITO-coated glass substrates (1.5 × 1.5 cm^2) were ultrasonically cleaned in detergent, deionized water, acetone, and isopropyl alcohol. After routine solvent cleaning, the substrates were treated with UV ozone for 15 min. Then, a modified ITO surface was obtained by spin coating a layer of poly(ethylene dioxythiophene):polystyrenesulfonate (PEDOT:PSS) (~30 nm). After baking at 130 °C for 1 h, the substrates were transferred to a nitrogen-filled glove box. Then,

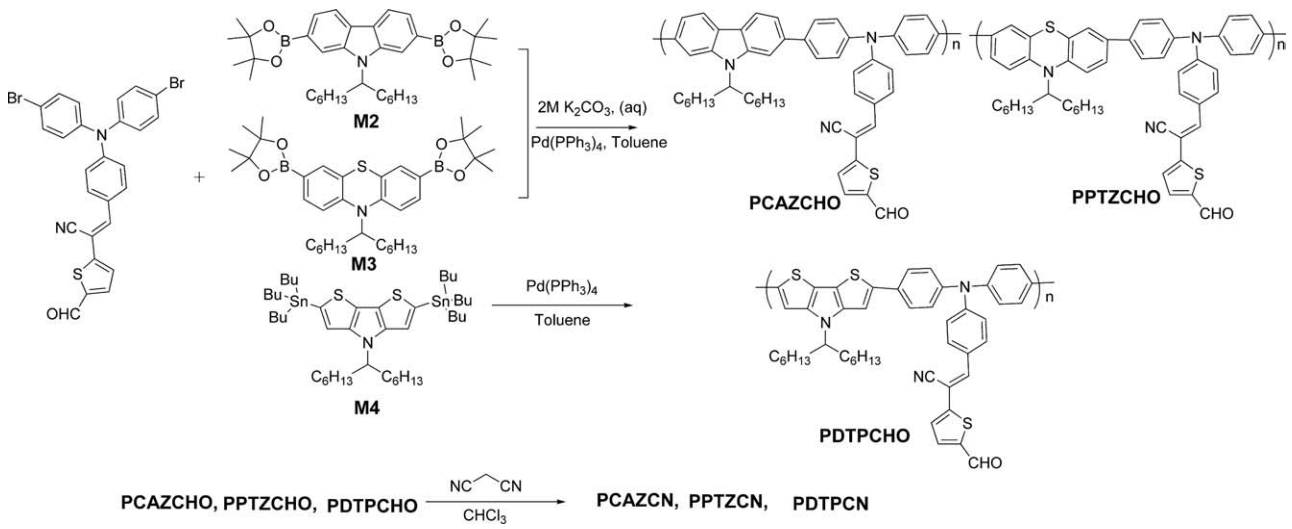

SCHEME 2 Synthetic routes of polymers (**PCAZCN**, **PPTZCN**, and **PDTPCN**).

on the top of PEDOT:PSS layer, the active layer was prepared by spin coating from blended solutions of polymer blends polymer:$PC_{61}BM$ (with 1:1 w/w) and **PCAZCN**:$PC_{71}BM$ (with 1:1, 1:2, 1:3, and 1:4 w/w) subsequently with a spin rate about 1000 rpm for 60 s, and the thickness of the active layer was typically about 80 nm. Initially, the blended solutions were prepared by dissolving both polymers and PCBM in 1,2 dichlorobenzene (20 mg/1 mL), followed by continuous stirring for 12 h at 50 °C. In the slow-growth approach, blended polymers in solid films were kept in the liquid phase after spin coating by using the solvent with a high boiling point. Finally, a calcium layer (30 nm) and a subsequent aluminum layer (100 nm) were thermally evaporated through a shadow mask at a pressure below 6×10^{-6} Torr. The active area of the device was 0.12 cm^2. All PSC devices were prepared and measured under ambient conditions. The solar cell measurements were done inside a glove box under simulated AM 1.5G irradiation (100 mW/cm^2) using a Xenon lamp-based solar simulator (Thermal Oriel 1000 W). The external quantum efficiency (EQE) spectra were obtained at short-circuit conditions. The light source was a 450 W Xe lamp (Oriel Instrument, model 6266) equipped with a water-based IR filter (Oriel Instrument, model 6123NS). The light output from the monochromator (Oriel Instrument, model 74100) was focused on the photovoltaic cell under test.

Fabrication of Hole- and Electron-Only Devices

The hole- and electron-only devices in this study contain polymer blends polymer:$PC_{61}BM$ (1:1) blend films sandwiched between transparent ITO anode and cathode. The devices have been prepared following the same procedure as the fabrication of BHJ devices, except that in the hole-only devices, Ca was replaced with MoO_3 (with work function $\Phi = 5.3$ eV) and for the electron-only devices, the PEDOT:PSS layer was replaced with Cs_2CO_3 (with work function $\Phi = 2.9$ eV). In hole-only devices, MoO_3 was thermally evaporated with a thickness of 20 nm and then capped with 50 nm of Al on the top of the active layer. On the other hand, Cs_2CO_3 was thermally evaporated in the electron-only devices with a thickness of ~2 nm on the top of transparent ITO. For both devices, annealing of the active layer was performed at 130 °C for 20 min.

Synthesis of Monomers (M1–M4) and Polymers (PCAZCN, PPTZCN, and PDTPCN)

The synthetic procedures of the monomers (**M1–M4**) and polymers (**PCAZCN, PPTZCN,** and **PDTPCN**) are given below, and the other intermediates are described in the Supporting Information.

3-(4-(Bis(4-bromophenyl)amino)phenyl)-2-(5-formylthiophen-2-yl)acrylonitrile (M1)

Phosphorousoxychloride (0.45 mL, 4.8 mmol) was added to a solution of 3-(4-(bis(4-bromophenyl)amino)phenyl)-2-(thiophen-2-yl)acrylonitrile (**1**) (2 g, 3.7 mmol) and DMF (0.5 mL, 6.5 mmol) in 1,2-dichloroethane (50 mL) cooled in an ice bath. The solution was then warmed up to room temperature and heated to reflux overnight. The reaction was cooled to room temperature and poured into a saturated aqueous sodium acetate solution (100 mL) and stirred for several hours to complete the hydrolysis. The reaction mixture was extracted with dichloromethane and washed with water, then the organic layer was dried over MgSO4, and concentrated in rotary evaporator. The crude product was purified by column chromatography (silica) using a mixture of hexane:ethyl acetate (10:1) as an eluent to yield a yellowish crystal (1.34 g, 64%).

^{1}H NMR (300 MHz, $CDCl_3$), δ (ppm): 9.90 (s, 1H), 8.02 (d, $J = 4.2$ Hz, 1H), 7.97 (s, 1H), 7.89 (d, $J = 8.7$ Hz, 2H), 7.57–7.54 (m, 5H), 7.08 (d, $J = 9$ Hz, 4H), 7.02 (d, $J = 8.7$ Hz, 2H). ^{13}C NMR (300 MHz, DMSO-d_6), δ (ppm): 182.7, 150.2, 149.1, 145.2, 142.7, 142.5, 137.2, 133.1, 131.6, 127.4, 127.3, 127.0, 126.3, 121.4, 118.1, 116.9, 102.2. MS (FAB): m/z [M^+]

563; calcd m/z [M^+] 561.94. Anal. Calcd for $C_{26}H_{16}Br_2N_2OS$: C, 55.34; H, 2.86; N, 4.96. Found: C, 55.41; H, 3.36; N, 4.92.

2,7-Bis(4,4,5,5-tetramethyl-1,3,2-dioxaborolan-2-yl)-9-(tridecan-7-yl)-9H-carbazole (M2)

A solution of compound **6** (3 g, 5.91 mmol) in anhydrous THF (80 mL) was cooled to −78 °C under nitrogen and stirred at this temperature for 5 min in the flame-dried two-necked round-bottom flask. *n*-Butyllithium (5.4 mL of 2.5 M solution in hexane, 13.6 mmol) was added dropwise, using a syringe, and the mixture was stirred at −78 °C for 1 h, then warmed up to 0 °C for 15 min, and cooled again to −78 °C. 2-Isopropoxy-4,4,5,5-tetramethyl-1,3,2-dioxaborolane (3.62 mL, 17.73 mmol) was added rapidly to the solution, and the resulting mixture was warmed to room temperature and stirred overnight. The reaction mixture was poured into water and extracted dichloromethane with a little brine wash. The organic extracts were dried over magnesium sulfate, and the solvent was removed by rotary evaporator. The obtained product was further purified by recrystallization from acetone to yield the title product as a white solid (2.56 g, 72.2%).

^{1}H NMR (300 MHz, $CDCl_3$), δ (ppm): 8.12 (br, 2H), 8.03 (br, 1H), 7.89 (br, 1H), 7.66 (d, J = 7.8 Hz, 2H), 4.70 (m, 1H), 2.35–2.31 (m, 2H), 1.98–1.92 (m, 2H), 1.39 (s, 24H), 1.05–0.95 (m, 16H), 0.78 (t, J = 6.6 Hz, 6H). ^{13}C NMR(300 MHz, $CDCl_3$), δ (ppm): 142.15, 138.91, 126.26, 124.81, 120.25, 118.31, 115.66, 83.91, 56.45, 34.03, 31.78, 29.33, 26.90, 25.15, 22.76, 14.22: m/z [M^+] 602; calcd m/z [M^+] 601.45. Anal. Calcd for $C_{37}H_{57}B_2NO_2$: C, 73.88; H, 9.55; N, 2.33. Found: C, 73.68; H, 9.68; N, 2.58.

3,7-Bis(4,4,5,5-tetramethyl-1,3,2-dioxaborolan-2-yl)-10-(tridecan-7-yl)-10H-phenothiazine (M3)

The monomer **M3** was synthesized by a similar procedure to that of **M2**, but the obtained product was purified by recrystallization from methanol to yield a white solid (yield: 74%).

^{1}H NMR (300 MHz, $CDCl_3$), δ (ppm): 7.53–7.50 (m, 4H), 6.86 (d, J = 8.1 Hz, 2H), 3.68 (m, 1H), 2.12–2.00 (m, 2H), 1.85–1.77 (m, 2H), 1.52–1.25 (m, 40H), 0.85 (t, J = 6.3 Hz, 6H). ^{13}C NMR (300 MHz, $CDCl_3$), δ (ppm): 147.95, 133.94, 133.88, 125.92, 116.85, 83.87, 64.44, 34.57, 31.90, 29.37, 27.61, 25.06, 22.75, 14.30: m/z [M^+] 634; calcd m/z [M^+] 633.42. Anal. Calcd for $C_{37}H_{57}B_2NO_4S$: C, 70.14; H, 9.07; N, 2.21. Found: C, 70.09; H, 9.03; N, 2.09.

2,6-Bis(tributylstannyl)-4-(tridecan-7-yl)-4H-dithieno[3,2-b:2′,3′-d]pyrrole (M4)

A solution of compound **9** (2 g, 5.53 mmol) in anhydrous THF (50 mL) was cooled to −78 °C under nitrogen and stirred at this temperature for 5 min in the flame-dried two-necked round-bottom flask. *n*-Butyllithium (4.6 mL of 2.5 M solution in hexane, 11.6 mmol) was added dropwise, using a syringe, and the mixture was stirred at −78 °C for 1 h, then warmed up to 0 °C for 15 min, and cooled again to −78 °C. Tri-*n*-butyltin chloride (3.30 mL, 12.17 mmol) was added rapidly to the solution, and the resulting mixture was warmed to room temperature and stirred overnight. The reaction mixture was poured into water and extracted with diethyl ether. The combined organic layers were washed with a little brine and dried over $MgSO_4$. After, the solvent had been removed under reduced pressure to afford **M4** (4.26 g, 82%).

^{1}H NMR (300 MHz, $CDCl_3$), δ (ppm): 6.97 (s, 2H), 4.26–4.22 (m, 1H), 2.03 (m, 2H), 1.87 (m, 2H), 1.64–1.59 (m, 12H), 1.41–1.12 (m, 40H), 0.96–0.86 (m, 24H). ^{13}C NMR (300 MHz, $CDCl_3$), δ (ppm): 143.90, 134.25, 122.07, 119.09, 59.83, 35.38, 31.78, 29.36, 28.05, 27.46, 27.34, 26.73, 22.75, 15.83, 14.20, 13.89, 11.13. m/z [M^+] 942; calcd m/z [M^+] 941.40. Anal. Calcd for $C_{45}H_{83}NS_2Sn_2$: C, 57.52; H, 8.90; N, 1.49. Found: C, 57.02; H, 9.20; N, 1.49.

Polymerization Procedures for Polymer Precursors PCAZCHO and PPTZCHO

Polymerization steps for **PCAZCHO** and **PPTZCHO** were carried out through the palladium(0)-catalyzed Suzuki coupling reactions. In a 50-mL flame-dried two-necked round-bottom flask, 1 equiv of **M1** and 1 equiv of **M2** or **M3** and $Pd(PPh_3)_4$ (1.5 mol %) were dissolved in a mixture of toluene (monomer = 0.5 M) and 2 M Na_2CO_3 (3:1). The solution was first put under a nitrogen atmosphere and vigorously stirred at 90–95 °C for 3 days. After reaction completion, an excess of bromobenzene was added to the reaction, and then 1 h later, excess of phenylboronic acid was added and the reaction refluxed overnight to complete the end-capping reaction. The polymer was purified by precipitation in methanol/water (10:1), filtered through 0.45-μm nylon filter, and washed on Soxhlet apparatus using hexane, acetone, and $CHCl_3$. The $CHCl_3$ fraction was reduced to 40–50 mL under reduced pressure, precipitated in methanol/water (10:1, 500 mL), filtered through 0.45-μm nylon filter, and finally air-dried overnight.

Poly[2-(5-formylthiophen-2-yl)-3-(4-(phenyl(4-(9-(tridecan-7-yl)-9H-carbazol-2-yl)phenyl)amino)phenyl)acrylonitrile] (PCAZCHO)

Dark black solid (yield: 76%). ^{1}H NMR (ppm, $CDCl_3$): δ 9.88 (s, 1H), 8.17 (m, 2H), 7.88–7.85 (m, 2H), 7.78–7.71 (m, 6H), 7.61 (s, 1H), 7.49 (m, 4H), 7.42–7.36 (m, 4H), 7.24–7.21 (m, 2H), 4.69 (m, 1H), 2.38 (m, 2H), 2.17 (m, 2H), 1.26–1.16 (m, 16H), 0.78 (t, J = 6.00 Hz, 6H). GPC (THF, polystyrene standard): M_n = 13,266 g/mol, M_w = 21,140 g/mol, PDI = 1.59.

Poly[2-(5-formylthiophen-2-yl)-3-(4-(phenyl(4-(10-(tridecan-7-yl)-10H-phenothiazin-3-yl)phenyl)amino)phenyl)acrylonitrile] (PPTZCHO)

Dark black solid (yield: 75%). ^{1}H NMR (300 MHz, $CDCl_3$), δ (ppm): 9.85 (s, 1H), 7.81–7.79 (m, 2H), 7.68 (s, 1H), 7.52–7.44 (m, 6H), 7.34 (m, 4H), 7.24–7.21 (m, 4H), 7.10–7.00 (m, 2H), 7.00–6.98 (m, 2H), 3.73 (m, 1H), 2.11 (m, 2H), 1.87 (m, 2H), 1.58 (m, 4H), 1.27 (m, 12H), 0.85 (m, 6H). GPC (THF, polystyrene standard): M_n = 10,121 g/mol, M_w = 18,825 g/mol, PDI = 1.86.

Synthetic Procedure for Polymer Precursor PDTPCHO

Polymerization steps for PDTPCHO were carried out through the Stille reactions. In a 50-mL flame-dried two-necked

round-bottom flask, equimolar of **M1** (0.25 g, 0.44 mmol) and **M4** (0.42 g, 0.44 mmol) followed by $Pd(PPh_3)_4$ (1 mol %) were dissolved in 8 mL of dry toluene and deoxygenated with nitrogen for 30 min. The reaction mixture was stirred at 110 °C for 3 days, and then an excess amount of 2-bromothiophene was added to end cap the trimethylstannyl groups for 4 h. The reaction mixture was cooled to 40 °C and added slowly into a vigorously stirred mixture of methanol/acetone (3:1). The polymers were collected by filtration and reprecipitation from methanol. The crude polymers were further purified by washing with acetone and EA for 2 days in a Soxhlet apparatus to remove oligomers and catalyst residues.

Poly[2-(5-formylthiophen-2-yl)-3-(4-(phenyl(4-(4-(tridecan-7-yl)-4H-dithieno[3,2-b:2′,3′-d]pyrrol-2-yl)phenyl)amino)phenyl)acrylonitrile] (PDTPCHO)

Dark black solid (yield: 70%). ^{1}H NMR (300 MHz, $CDCl_3$), δ (ppm): 9.88 (s, 1H), 7.84–7.81 (m, 2H), 7.71–7.61 (m, 4H), 7.46 (s, 1H), 7.40–7.41 (m, 2H), 7.23–7.14 (m, 8H), 4.22 (m, 1H), 2.04 (m, 2H), 1.87 (m, 2H), 1.25–1.16 (m, 16H), 0.81 (m, 6H). GPC (THF, polystyrene standard): M_n = 5037 g/mol, M_w = 6760 g/mol, PDI= 1.34.

Synthetic Procedures for Polymers PCAZCN, PPTZCN, and PDTPCN

Poly[2-((5-(1-cyano-2-(4-(phenyl(4-(9-(tridecan-7-yl)-9H-carbazol-2-yl)phenyl)amino)phenyl)vinyl)thiophen-2-yl)methylene)malononitrile] (PCAZCN)

To a solution of **PCAZCHO** (200 mg, 0.26 mmol) and malononitrile (172 mg, 5.2 mmol) in 15 mL of $CHCl_3$, 0.2 mL of pyridine was added. The mixture solution was stirred overnight at room temperature, then the resulting mixture was poured into methanol, and the precipitate was filtered off and washed with water. The resulted black color polymer was purified by repeated precipitation from its THF solution to methanol (175 mg, 82%).

^{1}H NMR (300 MHz, $CDCl_3$), δ (ppm): 8.18 (m, 2H), 7.91–7.88 (m, 2H), 7.78–7.73 (m, 6H), 7.63 (s, 1H), 7.57 (s, 1H), 7.50–7.48 (m, 3H), 7.42–7.37 (m, 5H), 7.24–7.20 (m, 2H), 4.70 (m, 1H), 2.38 (m, 2H), 2.15 (m, 2H), 1.26–1.15 (m, 16H), 0.78 (t, J = 6.00 Hz, 6H). GPC (THF, polystyrene standard): M_n = 13,781 g/mol, M_w = 21,103 g/mol, PDI = 1.53. Anal. Calcd C, 80.86%; H, 6.41%; N, 8.73%. Found: C, 79.73%; H, 6.18%; N, 8.40%.

Poly(2-((5-(1-cyano-2-(4-(phenyl(4-(10-(tridecan-7-yl)-10H-phenothiazin-3yl)phenyl)amino)phenyl)vinyl)thiophen-2-yl)methylene)malononitrile) (PPTZCN)

The synthesis procedure for **PPTZCN** was followed using the same procedure as that of **PCAZCN**. After purification afforded a black solid (81%).

^{1}H NMR (300 MHz, $CDCl_3$), δ (ppm): 7.85–7.82 (m, 2H), 7.77 (s, 1H), 7.74 (s, 1H), 7.60–7.46 (m, 6H), 7.34 (m, 4H), 7.25–7.21 (m, 4H), 7.12–6.98 (m, 4H), 3.73 (m, 1H), 2.17 (m, 2H), 1.87 (m, 2H), 1.58 (m, 4H), 1.27 (m, 12H), 0.85 (m, 6H). GPC (THF, polystyrene standard): M_n = 10,503 g/mol, M_w = 19,010 g/mol, PDI=1.81. Anal. Calcd C, 77.75%; H, 6.16%; N, 8.40%. Found: C, 76.95%; H, 6.22%; N, 8.12%.

Poly(2-((5-(1-cyano-2-(4-(phenyl(4-(4-(tridecan-7-yl)-4H-dithieno[3,2-b:2′,3′-d]pyrrol-2-yl)phenyl)amino)phenyl)vinyl)thiophen-2-yl)methylene)malononitrile) (PDTPCN)

The synthesis procedure for **PDTPCN** was followed using the same procedure as **PCAZCN**. After purification afforded a black solid (76%).

^{1}H NMR (300 MHz, $CDCl_3$), δ (ppm): 7.88–7.85 (m, 2H), 7.79–7.76 (m, 2H), 7.66–7.60 (m, 4H), 7.55 (s, 1H), 7.48 (s, 1H), 7.24–7.08 (m, 8H), 4.23 (m, 1H), 2.04 (m, 2H), 1.88 (m, 2H), 1.25–1.11 (m, 16H), 0.81 (m, 6H). GPC (THF, polystyrene standard): M_n = 5237g/mol, M_w = 6820 g/mol, PDI= 1.30. Anal. Calcd C, 73.76%; H, 5.82%; N, 8.60%. Found: C, 72.29%; H, 5.82%; N, 8.28%.

RESULTS AND DISCUSSION

Synthesis and Structural Characterization

The general synthetic routes of monomers **M1–M4** and polymers (**PCAZCN, PPTZCN**, and **PDTPCN**) are shown in Schemes 1 and 2, respectively. Synthesis of 4-(tridecan-7-yl)-4H-dithieno[3,2-b:2′,3′-d]pyrrole (**9**)[8(c)] was reported by known literature procedures. Monomers (**M1–M4**) were satisfactorily characterized by ^{1}H NMR, ^{13}C NMR, MS spectroscopy, and elemental analyses. As shown in Scheme 2, polymer precursors **PCAZCHO** and **PPTZCHO** were prepared by the well-known Pd(0)-catalyzed Suzuki polymerization between triphenylamine dibromide monomer **M1** and diboronic esters of 2,7-carbazole (**M2**) and phenothiazine (**M3**), respectively, and polymer precursor **PDTPCHO** was synthesized by Pd(0)-catalyzed Stille polymerization between triphenylamine dibromide monomers **M1** and **M4**. Furthermore, to increase the stability of polymers, end-caping reactions were carried out on all polymers. The obtained polymers were further purified by washing on Soxhlet apparatus using hexane and acetone and later on extracted by $CHCl_3$. The $CHCl_3$ fraction was concentrated to 40–50 mL under reduced pressure, precipitated in methanol, filtered through 0.45-μm nylon filters, and finally dried under reduced pressure at room temperature. After purification and drying, all polymers were obtained as black solids in overall good yields (70–76%).

Condensations of aldehydes in polymer precursors **PCAZCHO**, **PPTZCHO**, and **PDTPCHO** with excess of malononitrile in $CHCl_3$ solutions in the presence of pyridine afforded the corresponding polymers **PCAZCN**, **PPTZCN**, and **PDTPCN** in excellent yields (76–82%; see Fig. 1).[11(b)] All final polymers (**PCAZCN**, **PPTZCN**, and **PDTPCN**) exhibited good solubilities in common organic solvents, such as THF, $CHCl_3$, toluene, and chlorobenzene at room temperature.

The molecular weights of polymers **PCAZCN**, **PPTZCN**, and **PDTPCN** were determined by GPC against monodisperse polystyrene standards in THF and are summarized in Table 1. The number-average molecular weights (M_n) and the weight-average molecular weights (M_w) obtained in all polymers were in the range of 5237–13,781 and 6820–21,103, respectively, with polydispersity indices (PDI = M_w/M_n) ranging 1.30–1.81. The thermal properties of these polymers

TABLE 1 Molecular Weights and Thermal Properties of Polymers

Polymer	M_n[a]	M_w[a]	PDI[a]	T_d (°C)[b]
PCAZCN	13,781	21,103	1.53	393
PPTZCN	10,503	19,010	1.81	385
PDTPCN	5,237	6,820	1.30	377

[a] Molecular weights and polydispersity were measured by GPC, using THF as an eluent, polystyrene as a standard. M_n, number-average molecular weight; M_w, weight-average molecular weight.
[b] Temperature (°C) at 5% weight loss measured by TGA at a heating rate of 20 °C/min under nitrogen.

determined by TGA are shown in Figure S1 of the Supporting Information and summarized in Table 1. The TGA thermograms of polymers **PCAZCN**, **PPTZCN**, and **PDTPCN** revealed the decomposition temperatures (T_d with 5% weight loss) at 393, 385, and 377 °C, respectively.

Optical Properties

The optical properties of these D-A polymers (**PCAZCN**, **PPTZCN**, and **PDTPCN**) were investigated by UV–vis spectroscopy in THF solutions as well as in solid films. Figure 2(a,b) shows the normalized UV–vis absorption spectra of polymers in THF solutions (10^{-6} M) and solid films, respectively, and the data are illustrated in Table 2. Polymer **PCAZCN** in solution showed two absorption peaks [see Fig. 2(a)], where one peak at 374 nm is attributed to the π–π^* transitions of their conjugated polymer backbones and another peak at 536 nm is correspondent to the ICT interactions between their polymer main chains and pendent acceptor groups.[21] In polymer **PPTZCN**, the high-energy π–π^* transition bands situated at 377and 459 nm are consistent with the reported phenothiazine-based homopolymers or copolymers.[27] The low-energy peak appeared at 525 nm is due to the ICT transitions occurring between their polymer main chains and pendent acceptor groups similar to that of **PCAZCN**. However, in case of polymer **PDTPCN**, both π–π^* transition and ICT transition bands overlapped and showed a single absorption peak at 437 nm and the ICT transition band tailed up to 700 nm. In contrast to those solution spectra of all D-A polymers (**PCAZCN**, **PPTZCN**, and **PDTPCN**) shown in Figure 2(b) and Table 2, the absorption spectra in solid films were red shifted (~17–61 nm) and broadened to longer wavelength region tailed up to 750 nm. These bathochromic shifts in solid films are attributed to the intermolecular interactions in the solid state, which indicate the efficient packing of the polymer backbones in solid films.[13] The optical bandgaps (E_g^{opt}) of polymers **PCAZCN**, **PPTZCN**, and **PDTPCN** calculated from the absorption onsets in the solid films ($\lambda_{onset,\ film}$) were in the range of 1.66–1.72 eV. These low bandgaps of polymers could be attributed to the additional ICT transitions from electron-rich main-chain donors to the pendent electron-acceptor cyano- and dicyano-vinyl

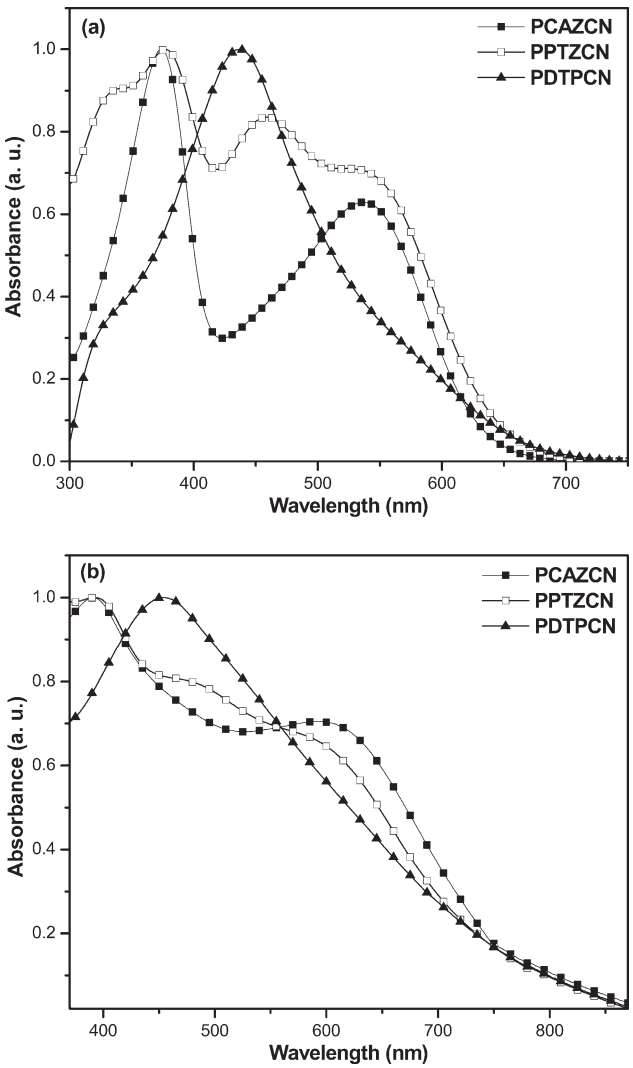

FIGURE 2 Normalized UV–vis spectra of polymers (**PCAZCN**, **PPTZCN**, and **PDTPCN**) in (a) dilute THF solutions (1×10^{-6} M) and (b) solid films.

TABLE 2 Optical Properties of Polymers

Polymer	$\lambda_{abs,\ sol}$ (nm)[a]	$\lambda_{abs,\ film}$ (nm)[b]	$\lambda_{onset,\ film}$ (nm)	E_g^{opt}, film (eV)[c]
PCAZCN	374, 536	391, 591	748	1.66
PPTZCN	377, 459, 525	393, 485, 586	729	1.70
PDTPCN	437	454	719	1.72

[a] In THF dilute solutions.
[b] Spin coated from THF solutions.
[c] The optical bandgaps were obtained from the equation E_g^{opt}, film = 1240/$\lambda_{onset,\ film}$.

TABLE 3 Electrochemical Properties of Polymers

Polymer	$E_{ox,onset}$ (V)[a]	$E_{red,onset}$ (V)[a]	HOMO (eV)[b]	LUMO (eV)[b]	E_g^{cv} (eV)
PCAZCN	0.97	−0.84	−5.32	−3.51	1.81
PPTZCN	0.85	−0.90	−5.20	−3.45	1.75
PDTPCN	0.77	−0.80	−5.12	−3.55	1.67

[a] Onset oxidation and reduction potentials measured by cyclic voltammetry in solid films.
[b] HOMO/LUMO = $[-(E_{onset} - 0.45) - 4.8]$ eV, where 0.45 V is the value for ferrocene versus Ag/Ag^+ and 4.8 eV is the energy level of ferrocene below the vacuum.

acceptors.[9–11,21] Among these polymers (**PCAZCN**, **PPTZCN**, and **PDTPCN**), **PCAZCN** has the broadest absorption spectrum toward a higher absorption wavelength attributed to a better packing of the polymer backbones, which leads to a more extensive delocalization of the electrons in the solid state.[13]

Electrochemical Properties

To understand the electronic structures of D-A polymers (**PCAZCN**, **PPTZCN**, and **PDTPCN**), the HOMO and LUMO levels were investigated by the CV measurements in solid films with Ag/AgCl as a reference electrode, calibrated by ferrocene ($E_{1/2(ferrocene)}$ = 0.45 mV vs. Ag/AgCl). The HOMO and LUMO levels were estimated by the oxidation and reduction potentials from the reference energy level of ferrocene (4.8 eV below the vacuum level) according to the following equation:[28] $E_{HOMO/LUMO} = [-(E_{onset} - 0.45) - 4.8]$ eV, and the results are summarized in Table 3. As shown in Figure S2 of the Supporting Information, all polymers **PCAZCN**, **PPTZCN**, and **PDTPCN** exhibited two quasi-reversible oxidations or p-doping/dedoping (oxidation/rereduction) processes with onset oxidation potentials ($E_{ox/onset}$) 0.97, 0.85, and 0.77 V, respectively. Nevertheless, the n-doping/dedoping (reduction/reoxidation) processes showed irreversible reduction potentials with onset reduction potentials ($E_{red/onset}$) of −0.84 V (**PCAZCN**), −0.90 V (**PPTZCN**), and −0.80 V (**PDTPCN**), respectively. On the basis of their corresponding $E_{ox/onset}$ and $E_{red/onset}$ values, the HOMO/LUMO levels of **PCAZCN**, **PPTZCN**, and **PDTPCN** were −5.32/−3.51, −5.20/−3.45, and −5.12/−3.55 eV, respectively. The obtained LUMO levels of the polymers were in the desirable range to afford efficient driving force for charge separation.[12] The data show that the different donor segments have almost no effects on the LUMO energy levels[20(b)] but affect the HOMO energy levels that are responsible for the V_{oc} values, which were reflected in the photovoltaic properties correspondingly.[12] In addition, the electrochemical bandgaps (E_g^{cv}) of **PCAZCN**, **PPTZCN**, and **PDTPCN** calculated from $E_g^{cv} = (E_{ox/onset} - E_{red/onset})$ were 1.81, 1.75, 1.67 eV, respectively, which lay within the acceptable range of errors to those obtained from their absorption spectra (E_g^{opt}).

Photovoltaic Properties

The potential applications of D-A polymers (**PCAZCN**, **PPTZCN**, and **PDTPCN**) in PSCs were explored by fabricating BHJ photovoltaic devices with a configuration of ITO/PEDOT:PSS (30 nm)/polymer:$PC_{61}BM$ blend (∼80 nm)/Ca(30 nm)/Al(100 nm). The polymer solutions for the active layer were prepared by blending polymers (**PCAZCN**, **PPTZCN**, and **PDTPCN**) and $PC_{61}BM$ in a weight ratio of 1:1 initially, and later the active-layer compositions were modified with various weight ratios of the previous optimum polymer blended with $PC_{71}BM$ (owing to a broader absorption and a higher absorption coefficient of $PC_{71}BM$ than $PC_{61}BM$). The *J–V* characteristics of the PSC devices based on polymers (**PCAZCN**, **PPTZCN**, and **PDTPCN**) and $PC_{61}BM$ (1:1 w/w) are shown in Figure 3, and the photovoltaic properties, that is, open circuit voltage (V_{oc}), short circuit current density (J_{sc}), fill factor (FF), and PCE values, are illustrated in Table 4. The V_{oc} values of polymers, which are dependent on the energy levels of the active-layer components,[18] correlate well with the cyclovoltometric results, that is, polymers with lower HOMO levels have higher V_{oc} values and vice versa. As a result, polymer **PCAZCN** has the highest V_{oc} value (0.79 V), and polymer **PDTPCN** has the lowest V_{oc} value (0.63 V). As shown in Figure 4, the absorbance spectra of polymer:$PC_{61}BM$ blend (1:1 w/w) in solid films measured from the PSC devices by using an ITO/PEDOT substrate as a reference were broadened toward longer wavelength region. Besides, the carrier transporting properties, that is, hole mobility (μ_h) and electron mobility (μ_e), of blended polymers in the active layer are also important parameters, which could affect the PCE values of PSC devices. To investigate the carrier transporting properties, which are accountable for the variation in FF and J_{sc} value in PSC devices,[29,30] the space charge limited current method[31] was used to evaluate μ_h and μ_e mobilities of polymer blends in polymer films of **PCAZCN**, **PPTZCN**, and **PDTPCN**:$PC_{61}BM$ (1:1 w/w), and the data are listed in Table 4. It is perceptible that, compared with **PPTZCN** ($\mu_e = 2.7 \times 10^{-8}$ cm^2/V s and $\mu_h = 3.6 \times 10^{-9}$ cm^2/V s) and **PDTPCN** ($\mu_e = 2.2 \times 10^{-8}$ cm^2/V s and $\mu_h = 2.7 \times 10^{-9}$ cm^2/V s), the hole and electron mobilities

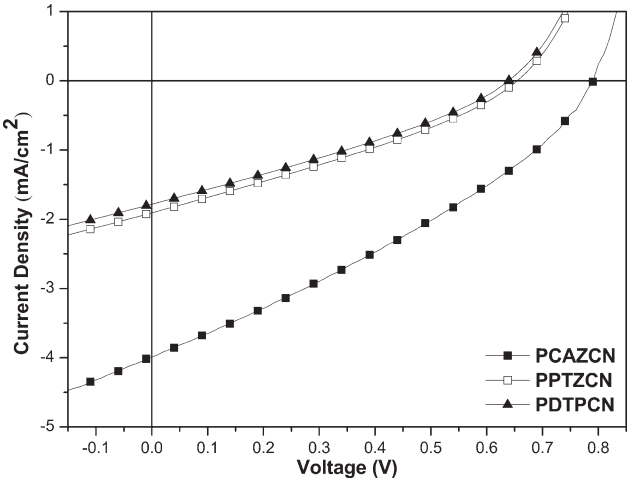

FIGURE 3 Current–voltage (*J–V*) curves of polymer solar cells containing polymer blends polymer:$PC_{61}BM$ = 1:1 (w/w) under the illumination of AM 1.5G, 100 mW/cm^2.

TABLE 4 Photovoltaic Properties of Polymer Solar Cell Devices with a Configuration of ITO/PEDOT:PSS/Polymer:$PC_{61}BM$/Ca/Al[a]

Polymer/ $PC_{61}BM$ (1:1)	μ_e (cm^2/V s)	μ_h (cm^2/V s)	V_{oc} (V)	J_{sc} (mA/cm^2)	FF (%)	PCE (%)
PCAZCN	5.8×10^{-8}	7.4×10^{-9}	0.79	3.99	32.0	1.01
PPTZCN	2.7×10^{-8}	3.6×10^{-9}	0.65	1.91	30.6	0.38
PDTPCN	2.2×10^{-8}	2.7×10^{-9}	0.63	1.78	30.3	0.34

[a] Measured under AM 1.5 irradiation, 100 mW/cm^2.

of **PCAZCN** ($\mu_e = 5.8 \times 10^{-8}$ cm^2/V s and $\mu_h = 7.4 \times 10^{-9}$ cm^2/V s) were much higher to induce larger J_{sc} (3.99 mA/cm^2) and FF (32.0%) values. The poor FF values of all polymers might be attributed to the possibility of recombination of holes and electrons in these polymers.[20(d)] The stronger and broader absorption spectrum at 550–650 nm of **PCAZCN**:$PC_{61}BM$ in the active layer (Fig. 4) increased its photocurrent response, and thus to show a broader and higher EQE value of ~11% (see Fig. S3 of the Supporting Information). Therefore, the device containing **PCAZCN**:$PC_{61}BM$ showed the highest J_{sc} value (3.99 mA/cm^2), which was larger than those of the devices containing **PPTZCN**:$PC_{61}BM$ (1.91 mA/cm^2) and **PDTPCN**:$PC_{61}BM$ (1.78 mA/cm^2).[21(b)] According to the atomic force microscopy (AFM) images of Supporting Information Figure S4, it was observed that a highest J_{sc} value (3.99 mA/cm^2) was induced in the device of **PCAZCN**:$PC_{61}BM$ (1:1 w/w) having the smoothest surface with a root-mean-square roughness (Rrms) of 0.26 nm, and J_{sc} values were reduced to 1.91 and 1.78 mA/cm^2 by increasing the roughness of **PPTZCN**:$PC_{61}BM$ (Rrms = 0.28 nm) and **PDTPCN**:$PC_{61}BM$ (Rrms = 0.36 nm), respectively. This is due to the large-scaled phase separation, which decreased the diffusional escape probabilities for mobile charge carriers, and hence to increase the charge recombination, which is fully consistent with the J_{sc} and PCE values obtained by the copolymers.[9(e,f)] On the basis of the above reasonable facts, the PSC device containing polymer **PCAZCN** as an electron donor and $PC_{61}BM$ as an electron acceptor (with 1:1 weight ratio) showed the best performance of a highest PCE = 1.01% with V_{oc} = 0.79 V, J_{sc} = 3.99 mA/cm^2, and FF = 32.0%. However, because of the poor dissociation of excitons at the polymer/acceptor interface and transport of free charge carriers toward the collecting electrodes,[30] the PCE values of **PPTZCN** (0.38%) and **PDTPCN** (0.34%) decreased significantly. The best performance of the PSC devices containing polymer **PCAZCN** was optimized by fabricating BHJ PSC devices using **PCAZCN** as a donor and $PC_{71}BM$ as an acceptor in different weight ratios of 1:1, 1:2, 1:3, and 1:4. The *J*–*V* curves and EQE curves of the PSC devices based on **PCAZCN**:$PC_{71}BM$ in four different blended ratios (1:1, 1:2, 1:3, and 1:4) are shown in Figures 5 and 6, respectively, and data are illustrated in Table 5. The PSC device based on **PCAZCN**:$PC_{71}BM$ in 1:2 weight ratio obtained the best PCE value of 1.28% with V_{oc} = 0.81 V, J_{sc} = 4.93 mA/cm^2, and FF = 32.1%. Indeed, the weight ratios between polymer donors and PCBM acceptor played a key role in all PCE values.[6(a),32] As shown in Table 5, because of the poor interfacial contacts between the donor polymers and $PC_{71}BM$

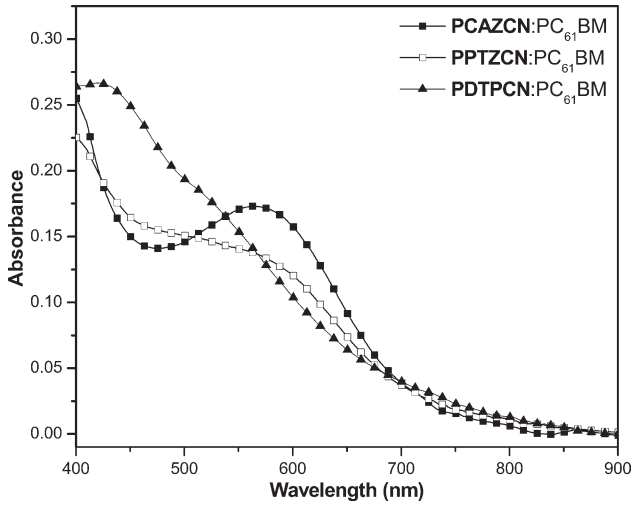

FIGURE 4 Absorption spectra of polymer blends of polymer:$PC_{61}BM$ = 1:1 (w/w) measured from solar cell devices by using the substrate of ITO/PEDOT as a reference.

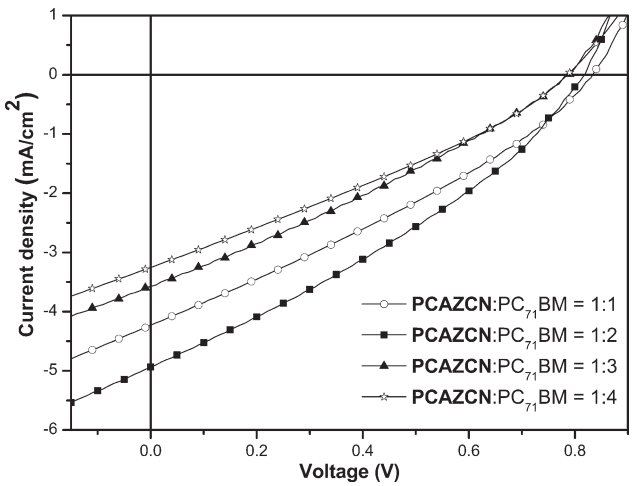

FIGURE 5 Current–voltage (*J*–*V*) curves of polymer solar cells containing polymer blends **PCAZCN**:$PC_{71}BM$ in different weight ratios under the illumination of AM 1.5G, 100 mW/cm^2.

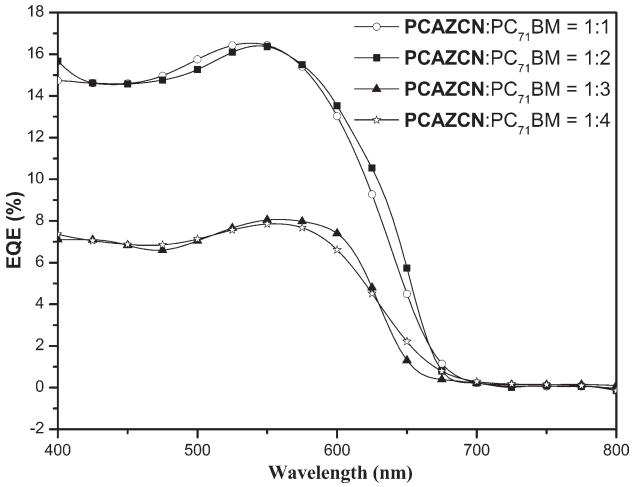

FIGURE 6 External quantum efficiency (EQE) of polymer solar cells containing polymer blends **PCAZCN**:$PC_{71}BM$ in different weight ratios.

TABLE 5 Photovoltaic Properties of Polymer Solar Cell Devices with a Configuration of ITO/PEDOT:PSS/**PCAZCN**:$PC_{71}BM$/Ca/Al[a]

PCAZCN:$PC_{71}BM$	V_{oc} (V)	J_{sc} (mA/cm^2)	FF (%)	PCE (%)
1:1	0.83	4.23	30.5	1.07
1:2	0.81	4.93	32.1	1.28
1:3	0.78	3.57	29.4	0.82
1:4	0.78	3.25	29.6	0.75

[a] Measured under AM 1.5 irradiation, 100 mW/cm^2.

acceptor, the other polymer blends of **PCAZCN**:$PC_{71}BM$ = 1:3 and 1:4 (w/w) with higher PCBM contents offered much lower PCE values (see Table 5), which led to the suppression of charge separation/transportation within the active layer.[33] Figure 6 shows EQE curves of PSC devices containing polymer **PCAZCN** in different weight ratios of **PCAZCN**:$PC_{71}BM$ = 1:1, 1:2, 1:3, and 1:4. The photocurrent responses displayed a maximum EQE value of ~17% at ~550 nm (at **PCAZCN**:$PC_{71}BM$ = 1:1 and 1:2 w/w), which are correspondent to that of the absorbance spectra of polymer blends in solid films measured from the PSC devices (see Fig. 4). The similarities between the absorption spectrum and EQE of polymer blend containing **PCAZCN** indicate that the photogeneration of charges originates predominantly

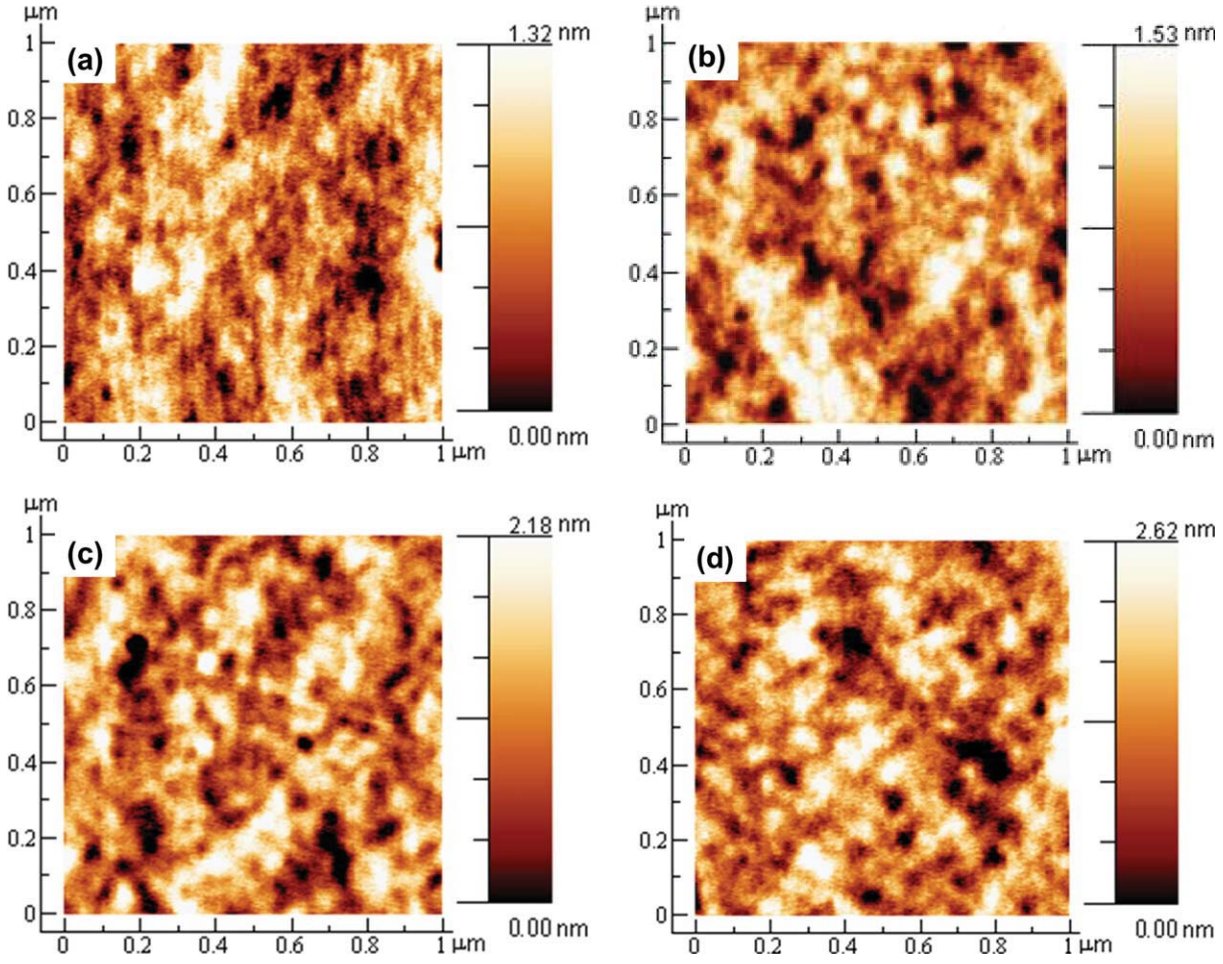

FIGURE 7 AFM images of polymer blends **PCAZCN**: $PC_{71}BM$ in different weight ratios. (a) 1:1 (w/w), (b) 1:2 (w/w), (c) 1:3 (w/w), and (d) 1:4 (w/w).

following the absorption of light by polymer.[6(a),32] It is worth noticing that the EQE values remain almost same for PSC devices containing **PCAZCN**:$PC_{71}BM$ = 1:1 and 1:2 (w/w). However, the EQE values decreased significantly by increasing the $PC_{71}BM$ proportion, which is likely due to the increase in imbalance of charge carrier mobilities at higher $PC_{71}BM$ concentrations.[14] Therefore, as shown in Table 5, the PCE values as well as FF and J_{sc} values of PSC devices containing **PCAZCN**:$PC_{71}BM$ in 1:3 and 1:4 (w/w) decreased correspondingly compared with that in 1:1 and 1:2 (w/w). In addition, the behavior of the photovoltaic properties can be well analyzed from the surface topography of the active layer. The AFM images of polymer blends **PCAZCN**:$PC_{71}BM$ as cast films in different weight ratios are given in Figure 7. The average Rrms of **PCAZCN**:$PC_{71}BM$ = 1:1, 1:2, 1:3, and 1:4 (w/w) were 0.17, 0.16, 0.18, and 0.21 nm, respectively, which indicates that the smoother surface has a higher PCE value ascribed to the better solubility and interfacial contacts of the polymer blend.

CONCLUSIONS

A series of novel low-bandgap conjugated triphenylamine-based polymers (**PCAZCN**, **PPTZCN**, and **PDTPCN**) consisting of different electron-rich donors (including 2,7-carbazole, phenothiazine, and dithianopyrol) in the main chains along with cyano- and dicyano-vinyl acceptors in the side chains were designed and copolymerized successfully by Pd(0)-catalyzed Suzuki or Stille coupling reaction. The electron-rich donor groups including triphenylamine in the polymer main chains endowed with strong and broad absorptions to get superior harvesting of sunlight and tunable HOMO levels and the electron-withdrawing cyano- and dicyano-vinyl in the side chains effectively reduced the bandgaps. The BHJ PSC device containing electron-donor polymer **PCAZCN** (bearing 2,7-carbazole units) and electron-acceptor $PC_{71}BM$ in 1:2 weight ratio afforded the highest PCE value of 1.28% with V_{oc} = 0.81 V, J_{sc} = 4.93 mA/cm^2, and FF = 32.1%. However, because of poor carrier transporting characteristics of **PPTZCN** and **PDTPCN**, their PCE values were reduced significantly.

The authors are grateful to the National Center for High-Performance Computing for computer time and facilities. The financial supports of this project provided by the National Science Council of Taiwan (ROC) through NSC 97-2113-M-009-006-MY2, National Chiao Tung University through 97W807, and Energy and Environmental Laboratories (charged by Chang-Chung Yang) in Industrial Technology Research Institute (ITRI) are acknowledged.

REFERENCES AND NOTES

1 (a) Yu, G.; Gao, J.; Hummelen, J. C.; Wudl, F.; Heeger, A. J. Science; 1995, 270, 1789–1791; (b) Gnes, S.; Neugebauer, H.; Sariciftci, N. S. Chem Rev 2007, 107, 1324–1338; (c) Brabec, C. J.; Sariciftci, N. S.; Hummelen, J. C. Adv Funct Mater 2001, 11, 15–26.

2 (a) Liang, Y. Y.; Wu, Y.; Feng, D. Q.; Tsai, S. T.; Son, H. J.; Li, G.; Yu, L. P. J Am Chem Soc 2009, 131, 56–57; (b) Liang, Y. Y.; Feng, D. Q.; Wu, Y.; Tsai, S. T.; Li, G.; Ray, C.; Yu, L. P. J Am Chem Soc 2009, 131, 7792–7799.

3 (a) Park, S. H.; Roy, A.; Beaupre, S.; Cho, S.; Coates, N.; Moon, J. S.; Moses, D.; Leclerc, M.; Lee, K.; Heeger, A. J. Nat Photon 2009, 3, 297–303; (b) Hou, J. H.; Chen, H. Y.; Zhang, S. Q.; Chen, R. I.; Yang, Y.; Wu, Y.; Li, G. J Am Chem Soc 2009, 131, 15586–15587.

4 Chen, H.-Y.; Hou, J.; Zhang, S.; Liang, Y.; Yang, G.; Yang, Y.; Yu, L.; Wu, L.; Li, G. Nat Photonics 2009, 3, 649–653.

5 (a) Krebs, F. C. Sol Energy Mater Sol Cells 2008, 92, 715–726; (b) Jørgensen, M.; Norrman, K.; Krebs, F. C. Sol Energy Mater Sol Cells 2008, 92, 686–714; (c) Hauch, J. A.; Schilinsky, P.; Choulis, S. A.; Childers, R.; Biele, M.; Brabec, C. J. Sol Energy Mater Sol Cells 2008, 92, 727–731; (d) Gevorgyan, S. A.; Krebs, F. C. Chem Mater 2008, 20, 4386–4390.

6 (a) Yi, H.; Johnson, R. G.; Iraqi, A.; Mohamad, D.; Royce, R.; Lidzey, D. G. Macromol Rapid Commun 2008, 29, 1804–1809; (b) Blouin, N.; Michaud, A.; Leclerc, M. Adv Mater 2007, 19, 2295–2300; (c) Zou, Y.; Gendron, D.; Aïch, R. B.; Najari, A.; Tao, Y.; Leclerc, M. Macromolecules 2009, 42, 2891–2894; (e) Blouin, N.; Michaud, A.; Gendron, D.; Wakim, S.; Blair, E.; Neaguplesu, R.; Belletete, M.; Durocher, G.; Tao, Y.; Leclerc, M. J Am Chem Soc 2008, 130, 732–742; (f) Mohamad, D.; Johnson, R. G.; Janeliunas, D.; Kirkus, M.; Yi, H.; Lidzey, D. G.; Iraqi, A. J Mater Chem 2010, 20, 6990–6997.

7 (a) Li, K.-C.; Huang, J.-H.; Hsu, Y.-C.; Huang, P.-J.; Chu, C.-W.; Lin, J.-T.; Ho, K.-C.; Wei, K.-H.; Lin, H.-C. Macromolecules 2009, 42, 3681–3693; (b) Tsai, J.-H.; Chueh, C.-C.; Chen, W.-C.; Yu, C.-Y.; Hwang, G.-W.; Ting, C.; Chen, E.-C.; Meng, H.-F. J Polym Sci Part A: Polym Chem 2010, 48, 2351–2360; (c) Jung, I. H.; Kim, H.; Park, M.-J.; Kim, B.; Park, J.-H.; Jeong, E.; Woo, H. Y.; Yoo, S.; Shim, H.-K. J Polym Sci Part A: Polym Chem 2010, 48, 1423–1432; (d) Peet, J.; Kim, J. Y.; Coates, N. E.; Ma, W. L.; Moses, D.; Heeger, A. J.; Bazan, G. C. Nat Mater 2007, 6, 497–500; (e) Li, K. C.; Hsu, Y.-C.; Lin, J.-T.; Yang, C.-C.; Wei, K. W.; Lin, H.-C. J Polym Sci Part A: Polym Chem 2009, 47, 2073–2092.

8 (a) Zhou, E.; Nakamura, M.; Nishizawa, T.; Zhang, Y.; Wei, Q.; Tajima, K.; Yang, C.; Hashimoto, K. Macromolecules 2008, 41, 8302–8305; (b) Zhou, E.; Wei, Q.; Yamakawa, S.; Zhang, Y.; Tajima, K.; Yang, C.; Hashimoto, K. Macromolecules 2010, 21, 821–826; (c) Yue, W.; Zhao, Y.; Shao, S.; Tian, H.; Xie, Z.; Geng, Y.; Wang, F. J Mater Chem 2009, 19, 2199–2206; (d) Liao, L.; Dai, L.; Smith, A.; Durstock, M.; Lu, J.; Ding, J.; Tao, Y. Macromolecules 2007, 40, 9406–9412; (e) Hou, J.; Chen, H.-Y.; Zhang, S.; Li, G.; Yang, Y. J Am Chem Soc 2008, 130, 16144–16145; (f) Huo, L.; Chen, H.-Y.; Hou, J.; Chen, T. L.; Yang, Y. Chem Commun 2009, 5570–5572; (g) Zhang, S.; He, C.; Liu, Y.; Zhan, X.; Chen, J. Polymer 2009, 50, 3595–3599.

9 (a) Mammo, W.; Admassie, S.; Gadisa, A.; Zhang, F.; Inganäs, O.; Andersson, M. R. Sol Energy Mater Sol Cells 2007, 91, 1010–1018; (b) Sun, M.; Wang, L.; Zhu, X.; Du, B.; Liu, R.; Yang, W.; Cao, Y. Sol Energy Mater Sol Cells 2007, 91, 1681–1687; (c) Li, K.-C.; Hsu, Y.-C.; Lin, J.-T.; Yang, C.-C.; Wei, K. W.; Lin, H.-C. J Polym Sci Part A: Polym Chem 2008, 46, 4285–4304; (d) Tang, W. H.; Kietzke, T.; Vemulamada, P.; Chen, Z. K. J Polym Sci Part A: Polym Chem 2007, 45, 5266–5276; (e) Li, Y. W.; Xue, L.

L.; Li, H.; Li, Z. F.; Xu, B.; Wen, S. P.; Tian, W. Macromolecules 2009, 42, 4491–4499; (f) Li, Y.; Li, H.; Xu, B.; Li, Z.; Chen, F.; Feng, D.; Zhang, J.; Tian, W. Polymer 2010, 51, 1786–1795.

10 (a) Li, Y.; Xue, L.; Xia, H.; Xu, B.; Wen, S.; Tian, W. J Polym Sci Part A: Polym Chem 2008, 46, 3970–3984; (b) Xue, L.; He, J.; Gu, X.; Yang, Z.; Xu, B.; Tian, W. J Phys Chem C 2009, 113, 12911–12917.

11 (a) Peng, Q.; Park, K.; Lin, T.; Durstock, M.; Dai, L. J Phys Chem B 2008, 112, 2801–2808; (b) Xia, P. F.; Feng, X. J.; Lu, J.; Tsang, S.-W.; Movileanu, R.; Tao, Y.; Wong, M. S. Adv Mater 2008, 20, 4810–4815.

12 Brédas, J.-L.; Beljonne, D.; Coropceanu, V.; Cornil, J. Chem Rev 2004, 104, 4971–5003.

13 Zou, Y.; Gendron, D.; Neagu-Plesu, R.; Leclerc, M. Macromolecules 2009, 42, 6361–6365.

14 (a) Chappell, J.; Lidzey, D. G.; Jukes, P. C.; Higgins, A. M.; Thompson, R. L.; O'Connor, S.; Grizzi, I.; Fletcher, R.; O'Brien, J.; Geoghegan, M.; Jones, R. A. L. Nat Mater 2003, 2, 616–621.

15 Huo, L.; Hou, J.; Chen, H.-Y.; Zhang, S.; Jiang, Y.; Chen, T. L.; Yang, Y. Macromolecules 2009, 42, 6564–6571.

16 (a) Chen, H.-Y.; Hou, J.; Hayden, A. E.; Yang, H.; Houk, K. N.; Yang, Y. Adv Mater 2010, 22, 371–375; (b) Zhang, F.; Bijleveld, J.; Perzon, E.; Tvingstedt, K.; Barrau, S.; Inganäs, O.; Andersson, M. R. J Mater Chem 2008, 18, 5468–5474.

17 (a) Huang, J.; Wu, Y.; Fu, H.; Zhan, X.; Yao, J.; Barlow, S.; Marder, S. R. J Phys Chem A 2009, 113, 5039–5046; (b) Zhan, X.; Tan, Z.; Domercq, B.; An, Z.; Zhang, X.; Barlow, S.; Li, Y.; Zhu, D.; Kippelen, B.; Marder, S. R. J Am Chem Soc 2007, 129, 7246–7247; (c) Chen, R.-T.; Chen, S.-H.; Hsieh, B.-Y.; Chen, Y. J Polym Sci Part A: Polym Chem 2009, 47, 2821–2834.

18 Scharber, M. C.; Muhlbacher, D.; Koppe, M.; Denk, P.; Waldauf, C.; Heeger, A. J.; Brabec, C. J. Adv Mater 2006, 18, 789–794.

19 Chen, X.; Schulz, G. L.; Han, X.; Zhou, Z.; Holdcroft, S. J Phys Chem C 2009, 113, 8505–8512.

20 (a) Cheng, Y. J.; Yang, S. H.; Hsu, C. S. Chem Rev 2009, 109, 5868–5923; (b) Zhou, E.; Yamakawa, S.; Tajima, K.; Yang, C.; Hashimoto, K. Chem Mater 2009, 21, 4055–4061; (c) Zhou, E.; Cong, J.; Yamakawa, S.; Wei, Q.; Nakamura, M.; Tajima, K.; Yang, C.; Hashimoto, K. Macromolecules 2010, 43, 2873–2879; (d) Li, Y.; Li, Z.; Wang, C.; Li, H.; Lu, H.; Xu, B.; Tian, W. J Polym Sci Part A: Polym Chem 2010, 48, 2765–2776; (e) Jung, I. H.; Yu, J.; Jeong, E.; Kim, J.; Kwon, S.; Kong, H.; Lee, K.; Woo, H. Y.; Shim, H.-K. Chem Eur J 2010, 16, 3743–3752.

21 (a) Huang, F.; Chen, K.-S.; Yip, H.-L.; Hau, S. K.; Acton, O.; Zhang, Y.; Luo, J.; Jen, A. K.-Y. J Am Chem Soc 2009, 131, 13886–13887; (b) Duan, C.; Cai, W.; Huang, F.; Zhang, J.; Wang, M.; Yang, T.; Zhong, C.; Gong, X.; Cao, Y. Macromolecules 2010, 43, 5262–5268; (c) Zhang, Z.-G.; Zhang, K.-L.; Liu, G.; Zhu, C.-X.; Neoh, K.-G.; Kang, E.-T. Macromolecules 2009, 42, 3104–3111; (d) Chang, Y.-T.; Hsu, S.-L.; Chen, G.-Y.; Su, M.-H.; Singh, T. A.; Diau, E. W.-G.; Wei, K.-H. Adv Funct Mater 2008, 18, 2356–2365; (e) Koyuncu, S.; Zafer, C.; Koyuncu, F. B.; Aydin, B.; Can, M.; Sefer, E.; Ozdemir, E.; Icli, S. J Polym Sci Part A: Polym Chem 2009, 47, 6280–6291.

22 (a) Zheng, Q.; Jung, B. J.; Sun, J.; Katz, H. E. J Am Chem Soc 2010, 132, 5394–5404; (b) Nguyen, L. H.; Hoppe, H.; Erb, T.; Gunes, S.; Gobsch, G.; Sariciftci, N. S. Adv Funct Mater 2007, 17, 1071–1078.

23 Halls, J. J. M.; Walsh, C. A.; Greenham, N. C.; Marseglla, E. A.; Friend, R. H.; Moratti, S. C.; Holmes, A. B. Nature 1995, 376, 498–500.

24 (a) Greenham, N. C.; Moratti, S. C.; Bradley, D. D. C.; Friend, R. H.; Holmes, A. B. Nature 1993, 365, 628–630; (b) Kraft, A.; Grimsdale, A. C.; Holmes, A. B. Angew Chem Int Ed 1998, 37, 402–428; (c) Li, H.; Hu, Y.; Zhang, Y.; Ma, D.; Wang, L.; Jing, X.; Wang, F. J Polym Sci Part A: Polym Chem 2004, 42, 3947–3953.

25 Liu, M. S.; Jiang, X. Z.; Liu, S.; Herguth, P.; Jen, A. K.-Y. Macromolecules 2002, 35, 3532–3538.

26 Chang, H.-W.; Lin, K. H.; Chueh, C.-C.; Liou, G.-S.; Chen, W.-C. J Polym Sci Part A: Polym Chem 2009, 47, 4037–4050.

27 (a) Park, M. J.; Lee, J.; Jung, I. H.; Park, J. H.; Hwang, D. H.; Shim, H. K. Macromolecules 2008, 41, 9643–9649; (b) Hwang, D.-H.; Kim, S.-K.; Park, M.-J.; Lee, J.-H.; Koo, B.-W.; Kang, I.-N.; Kim, S.-H.; Zyung, T. Chem Mater 2004, 16, 1298–1303.

28 (a) Yang, P.-J.; Wu, C.-W.; Sahu, D.; Lin, H.-C. Macromolecules 2008, 41, 9692–9703; (b) Liang, T.-C.; Chiang, I.-H.; Yang, P.-J.; Kekuda, D.; Chu, C.-W.; Lin, H.-C. J Polym Sci Part A: Polym Chem 2009, 47, 5998–6013.

29 Tan, M. J.; Goh, W.-P.; Li, J.; Pundir, G.; Chellappan, V.; Chen, Z.-K. ACS: Appl Mater Interfaces 2010, 2, 1414–1420.

30 (a) Savenije, T. J.; Kroeze, J. E.; Yang, X.; Loos, J. Adv Funct Mater 2005, 15, 1260–1266; (b) Baek, N. S.; Hau, S. K.; Yip, H. L.; Acton, O.; Chen, K. S.; Jen, A. K. Y. Chem Mater 2008, 20, 5734–5736; (c) Blom, P. W. M.; Mihailetchi, V. D.; Koster, L. J. A.; Markov, D. E. Adv Mater 2007, 19, 1551–1566.

31 (a) Malliaras, G. G.; Salem, J. R.; Brock, P. J.; Scott, C. Phys Rev B 1998, 58, 13411–13414; (b) Chirvase, D.; Chiguvare, Z.; Knipper, M.; Parisi, J.; Dyakonov, V.; Hummelen, J. C. Phys Rev B 2004, 70, 235207.

32 (a) Walker, B.; Tamayo, A. B.; Dang, X.-D.; Zalar, P.; Seo, J.-H.; Garcia, A.; Tantiwiwat, M.; Nguyen, T.-Q. Adv Funct Mater 2009, 19, 3063–3069.

33 (a) Dennler, G.; Scharber, M.; Brabec, C. J. Adv Mater 2009, 21, 1323–1338; (b) Cravino, A.; Sariciftci, N. S. J Mater Chem 2002, 12, 1931–1943.